HHS Public Access

Author manuscript

Pharm Res. Author manuscript; available in PMC 2016 October 01.

Published in final edited form as:

Pharm Res. 2015 October ; 32(10): 3269–3281. doi:10.1007/s11095-015-1703-5.

Across-Species Scaling of Monoclonal Antibody Pharmacokinetics Using a Minimal PBPK Model

Jie Zhao, **Yanguang Cao**, and **William J Jusko**

Department of Pharmaceutical Sciences, School of Pharmacy and Pharmaceutical Sciences, State University of New York at Buffalo, Buffalo, NY, 14214, USA. wjjusko@buffalo.edu

Abstract

Purpose—To examine the across-species scalability of monoclonal antibody (mAb) pharmacokinetics (PK) and assess similarities in tissue distribution across species using a recently developed minimal PBPK (mPBPK) model.

Methods—Twelve sets of antibody PK data from various species were obtained from the literature, which were jointly and individually analyzed. In joint analysis, vascular reflection coefficients for tissues with either tight (σ_1) or leaky endothelium (σ_2) were assumed consistent across species with systemic clearance allometrically scaled ($CL= a \cdot BW^b$). Four parameters (σ_1, σ_2, a, and b) were estimated in the joint analysis. In addition, the PK from each species was individually analyzed to assess species similarities in tissue distribution.

Results—Twelve mAb PK profiles were well-captured by the mPBPK model in the joint analysis. The estimated σ_1 ranged 0.690 to 0.999 with an average of 0.908; and σ_2 ranged 0.258 to 0.841 with an average of 0.579. Clearance was reasonably scaled and b ranged 0.695 to 1.27 averaging 0.91. Predictions of plasma concentrations for erlizumab and canakinumab in humans using parameters obtained from fitting animal data were consistent with actual measurements.

Conclusions—Therapeutic mAbs given *IV* usually exhibit biexponential kinetics with their distribution properties best captured using physiological concepts. The mPBPK modeling approach may facilitate efforts in translating antibody distribution and overall PK across species.

Keywords

Second-generation mPBPK; monoclonal antibody; allometric scaling

INTRODUCTION

Pharmacokinetic and pharmacodynamic (PK/PD) assessments play a critical role in the monoclonal antibody (mAb) discovery and development process (1). The PK/PD properties of antibody drugs are unique and largely different from small molecule drugs. Antibody drugs show several special properties, including limited vascular permeability, neonatal Fc receptor recycling, and more common receptor-mediated nonlinearity (2). Despite the

Supplementary Materials

Also provided are further references pertaining to the specific antibodies that were modeled and the Adapt computer code used for joint modeling of mAb profiles from two or more species.

complexity of mAb PK properties, a number of well-established methodologies are available for interspecies scaling of PK of mAb either from animals to humans or from one species to another (3,4).

There are three widely utilized approaches for anticipating mAb PK. Allometric scaling is the fundamental and most widely used approach, which is based on the assumption that different species have similarities in anatomy, physiology, and biochemistry (3). In many cases, mAb PK parameters, such as systemic clearance and volume of distribution at steady-state, have been scaled across species as a function of body weight with the relationship $Y = a \cdot BW^b$, where Y is the parameter of interest, BW is body weight, a is the allometric coefficient, and b is the allometric exponent (4, 5). Allometric scaling usually can provide good predictions of mAb PK in man if the assumption is valid that body weight alone determines all differences. This may not always be true (6). Some corrective factors have been applied accounting for additional differences in PK among species, such as brain weight, maximum life span potential, protein binding, or *in vitro* hepatocyte intrinsic *CL* (7-9). This approach often requires linear PK across species and sometimes is not applicable for mAbs that exhibit target-mediated nonlinear drug disposition.

Another approach for predicting mAbs PK in man based on animal data is the Dedrick approach (10), which applies physiological time to superimpose the concentration-time profiles of several species. This has been applied in projecting concentration-time profiles of mAbs in man reasonably well (1). An advantage of the Dedrick approach is that data from only one species is needed. Additionally, this approach could apply in a nonlinear system assuming that the Michaelis-Menten variables (K_m and V_{max}) are scalable or similar across species and differences of target expression among species are not taken into consideration (1).

Integrating fundamental allometric scaling principles into physiologically-based pharmacokinetic (PBPK) modeling provides an alternative and most advanced approach for PK interspecies scaling. Species-specific parameters [i.e., tissue volumes and blood flow rates] and drug specific information [i.e., tissue to plasma partition coefficients (K_p), protein binding parameters] are specified in the model building process (11). Once the model predicts PK behavior well in one species, it can be extended to other species by utilizing species-specific physiological information. A PBPK model was first applied to scale-up distribution of mAb from mice to man by Baxter *et al* (11, 12). The PBPK model produced good predictions of mAb disposition in man as well as tumor uptake by scaling murine parameters using known empirical relationships (13). Full PBPK models best integrate drug- and species-specific information providing prediction of PK parameters, tissue concentration versus time profiles, and providing more mechanistic insights into the properties of mAbs. However, full PBPK models for mAbs have limitations in regard to availability of tissue concentrations and the mathematical complexity of the model (14).

The targets of many therapeutic mAbs often exist in extravascular space, mostly in interstitial fluid (*ISF*). Antibody concentrations in *ISF* are directly associated with target engagement and efficacy. However, measuring mAb concentrations in *ISF* is technically challenging because of difficulties in sampling *ISF*. In such situations, PBPK models are

believed to be useful alternatives. Minimal PBPK models were recently developed to allow analysis of only plasma time-course data to reasonably predict antibody concentrations in *ISF* (15-17). Such models bridge compartmental and full PBPK models. They provide greater insight into mAb disposition and elimination with less complexity than a full PBPK model. More importantly, these models provide meaningful predictions of antibody distribution in two groups of lumped tissues.

This study evaluates the feasibility of integrating allometric principles into the basic minimal PBPK model to scale antibody PK across species and compare tissue bio-distribution. This model was used to jointly and individually analyze the PK of 12 antibodies across species, mainly to: 1) evaluate scalability using this model for mAb PK analysis, 2) demonstrate the feasibility of this model for predicting human PK as a general approach in species translation, and 3) compare antibody PK and tissue bio-distribution across species.

THEORETICAL

Second-generation mPBPK model integrated with allometric scaling

Allometric principles were incorporated into the basic second-generation mPBPK model (Figure 1). The model structure was described in our previous publications (15, 16). Tissues are divided into two compartments V_{tight} and V_{leaky} according to their tissue vascular endothelial structure. Muscle, skin, adipose, and brain are assigned as V_{tight}, whereas, liver, kidney, heart, and all other tissues are denoted as V_{leaky}. We assumed clearance from plasma. In joint analysis, vascular reflection coefficients for tissues with either tight (σ_1) or leaky endothelium (σ_2) were assumed consistent across species. The differential equations for the model are:

$$\frac{dC_p}{dt}=\frac{\text{Input}}{V_p}+\left[C_{\text{lymph}}\bullet L-C_p\bullet L_1\bullet(1-\sigma_1)-C_p\bullet L_2\bullet(1-\sigma_2)-\text{a}\bullet BW^b\right]/V_p \quad (1)$$

$$\frac{dC_{\text{tight}}}{dt}=\left[L_1\bullet(1-\sigma_1)\bullet C_p-L_1\bullet(1-\sigma_L)\bullet C_{\text{tight}}\right]/V_{\text{tight}} \quad (2)$$

$$\frac{dC_{\text{leaky}}}{dt}=\left[L_2\bullet(1-\sigma_2)\bullet C_p-L_2\bullet(1-\sigma_L)\bullet C_{\text{leaky}}\right]/V_{\text{leaky}} \quad (3)$$

$$\frac{dC_{\text{lymph}}}{dt}=\left[L_1\bullet(1-\sigma_L)\bullet C_{\text{tight}}+L_2\bullet(1-\sigma_L)\bullet C_{\text{leaky}}-C_{\text{lymph}}\bullet L\right]/V_{\text{lymph}} \quad (4)$$

where C_p is mAb concentration in V_p (plasma volume), C_{tight} and C_{leaky} refer to mAb concentration in V_{tight} and V_{leaky}, V_{lymph} is lymph volume, assumed equal to blood volume in this model, L_1 and L_2 are lymph flow for V_{tight} and V_{leaky}, and L is total lymph flow equal to the sum of L_1 and L_2 assuming $L_1 = 0.33{\cdot}L$ and $L_2 = 0.67{\cdot}L$. The relative fractions of lymph flow in the two types of tissues are believed to be constant across species. The σ_1 and σ_2 are vascular reflection coefficients for V_{tight} and V_{leaky} and we assume both σ_1 and $\sigma_2 < 1$. The σ_L is lymphatic capillary reflection coefficient, which is assigned to be 0.2 in this

model. We assumed clearance (CL_p) from plasma and allometric scaling of systemic clearance across species based on body weight (*BW*) with the allometric equation: $CL = a \cdot BW^b$, where *a* and *b* are allometric coefficients.

In this model, we used typical species-specific physiological values for body weight, plasma and tissue sizes, and lymph flows (*L*) and volumes (V_{lymph}). We assumed $V_{tight} = 0.65 \cdot ISF \cdot K_p$ and $V_{leaky} = 0.35 \cdot ISF \cdot K_p$, where *ISF* is total interstitial fluid. The K_p is available fraction of interstitial fluid for mAb distribution, which was assigned as 0.8 for native IgG_1 and 0.4 for native IgG_4 according to previous studies. The K_p was fixed 0.8 given the fact that most developed antibodies show similar isoelectric points with native IgG_1 (18). The relative fractions of V_{tight} and V_{leaky} to total *ISF* were calculated based upon the values used in full PBPK models (19). The relative fractions of *ISF* in V_{tight} and V_{leaky} were assumed to be constant across species. For joint analysis, we assumed that each mAb had the same vascular reflection coefficients for both tight tissues (σ_1) and leaky tissues (σ_2) among species. For individual fitting, we calculated each species' distribution rate, which also known as the transcapillary escape rate (*TER*) (20). *TER* is an essential factor to evaluate mAb distribution in extravascular spaces. *TER* is the sum of two routes, $TER = L_1 \cdot (1 - \sigma_1) + L_2 \cdot (1 - \sigma_2)$. The concentration ratio at equilibrium between *ISF* and plasma was calculated as $(1 - \sigma_1)/(1 - \sigma_L)$ for V_{tight} and $(1 - \sigma_2)/(1 - \sigma_L)$ for V_{leaky}.

For lymph flow, since no monkey value was available from the literature, we applied allometric scaling between lymph flow and body weights for the values from available species. The physiological parameters used for lymph flow scaling (21-23) and model fitting are listed in Table I.

Data analysis

The PK profiles of 12 mAbs in different species were analyzed using the mPBPK model (Table **II**). The rituximab PK in mice were in-house data. Data for other biologics in animals and man were digitized using Digitizer software (25): rituximab (S1,S2), dacetuzumab (S3), RSHZ19 (S4-6), bevacizumab (S7,S8), trebananib (S9,S10), belimumab (S11,S12), AB-01(S13,S14), erlizumab (S15,S16), canakinumab (S17), SB249417 (S18,S19), rilotumumab (S20,S21), and AB-02 (S14,S22). The mAbs selected were those with linear PK in the tested dose range and study conditions.

The PK data from different species were analyzed either jointly or individually. In joint analysis, all species were assumed to have common vascular reflection coefficients for both types of tissues (σ_1, σ_2) with *CL* allometrically scaled. This analysis was designed to assess the across-species scalabilities of the mPBPK parameters. With this approach, the plasma profiles of erlizumab and canakimumab in man were predicted and compared with experimental observations to evaluate model performance. The model-predicted *CL* for all these antibodies was further compared with that derived from non-compartmental analysis (*NCA*). The *NCA* was performed using Phoenix TM WinNonlin® 6.3 (Pharsight, Mountain View, CA). The concentration at time zero (C_0) was estimated via linear back extrapolation to time zero using the first two time points. Area under the concentration time curve from time zero to infinity (*AUC)* was calculated by the linear trapezoidal interpolation method. The slope of the apparent terminal phase was estimated by log-linear regression using

weighting with power -2. In individual analyses, the PK profiles for each species were separately analyzed with the mPBPK model to estimate species-specific vascular reflection coefficients by fixing allometric factors *a* and *b* that were obtained from jointly fitting data from all of the species for each antibody. This analysis evaluates the species differences of each mAb in tissue distribution and explores which species reveals the most similar distribution behaviors comparing values from man.

Model fitting was evaluated in terms of parameter estimates and several model performance criteria. Computer simulations were performed using ADAPT 5 and fittings utilized the maximum likelihood method in ADAPT 5 with naïve pooling data analysis (26). The variance model was defined as:

$$V_i = (\text{intercept} + \text{slope} \cdot Y(t_i))^2$$

where V_i is the variance of the response at the i_{th} time point, t_i is the actual time at the i_{th} time point, and $Y(t_i)$ is the predicted value at time t_i from the model. The variance parameter intercept and slope were estimated to together with system parameters. Model performance was evaluated by goodness of fitting with visual checks, sum-of-squared residuals, Akaike Information Criterion (*AIC*), Schwarz Criterion (*SC*), and Coefficient of Variation (*CV* %) of the estimated parameters.

RESULTS

The mAbs analyzed in this study are summarized in Table **II**. Data for 12 mAb and mAb derivatives include ten full antibodies, one mAb fragment, and one peptibody. One mAb is chimeric IgG, two mAb are human IgG, and eight mAb are humanized IgG. Allometric scaling was applied with four species for 2 mAb, three species for 5 mAbs, and two species for 5 mAbs. All mAb selected in this analysis showed linear PK that is usually analyzed with a two-compartment (2CM) mammillary model. The human data in this study, except for RSHZ19, canakinumab, and SB249147, were from healthy volunteers with the others from patients. We included all the species data available in the literature for rodent (eg, mouse, rat) and non-rodent species (eg, monkey, rabbit). Some studies showed that monkey is the most common species for PK analysis due to similar affinity of target binding for most mAbs in monkeys and man (27). Non-cross-reactive species, such as mouse and rat, have also been used for *CL* determination, particularly for nonspecific clearance (usually linear and not related to the binding with target antigen), which might be suitable for characterizing *CL* for mAbs showing linear kinetics (28). The mAbs selected in this analysis include 9 antibodies targeting soluble antigens and 3 for membrane-bound antigens.

Physiological parameters are important components for physiologically-based PK models. The physiological parameters used in lymph flow scaling and model fitting are shown in **Table I**. The lymph flow and volume of interstitial fluid are two critical physiological components in mAb PK analysis. However, directly measured lymph flow for each organ was not available, which necessitates two major assumptions: a) Lymph flow for each tissue is proportional to tissue blood flow (an assumption commonly used in full PBPK models) (29). This gives the fraction of lymph flow for V_{tight} as 0.33 ($L_1 = 0.33\cdot$) and for V_{tight} as

0.67 ($L_2 = 0.33 \cdot L$). b) Lymph flow through the thoracic duct measured by cannulation accounts for 80% of total lymph flow (23), and the percentage is conserved across species. Then, using the literature reported thoracic lymph flow, the total lymph flow was calculated (Table I). These values conform to an allometric relationship (Figure 2): *Lymph Flow* = $4.92 \cdot BW^{0.730}$. The total lymph flow for monkey was not available and thus predicted with this equation, and the lymph flow for other species in our model utilized the calculated total lymph flow (Table I).

For joint fitting, the PK profiles of 12 mAbs were well-captured by the mAb mPBPK model for various species resulting in estimates of parameters with high precision (*CV*% < 50%). The fitted profiles are shown in Figures 3 and 4 and the parameters are listed in **Table III**. In this analysis, we assumed that the parameters derived from the minimal PBPK model are either conserved (σ_1 and σ_2) or scalable across species (CL_p). These physiological components help to reveal the intrinsic factors that are closely related to drug properties and leave the species differences accounted for by physiological parameters. The low *CV%* values for the parameter estimates indicate good model performance, although fittings for some of the digitized data are only approximate.

The vascular reflection coefficients were quite consistent across species, but differed among the antibodies: σ_1 ranged 0.690 to 0.999 with an average of 0.908, σ_2 ranged 0.258 to 0.841 with an average of 0.579 (Figure 5). The estimated ranges of σ are consistent with our survey results of the PK of over 72 antibodies in man (16). In this model, the higher σ indicates greater vascular reflection and lower extravasation rate and extent. Thus, tissues with continuous endothelial vasculature exhibit lesser antibody distribution than tissues with fenestrated or discontinuous vasculature. This distributional feature of antibodies is consistent across species. The *CL* was reasonably scaled based on body weight. The range for *b* was 0.695 to 1.27 averaging 0.91 (Figure 5). This differs from the typical value of 0.75 that is commonly found for small molecules. Interestingly, this value is slightly greater than the commonly found value of 0.85 (30) based on scaling *NCA*-derived clearance (*CL = Dose/AUC*).

Comparisons of *CL* between *NCA* and mPBPK model fitting are listed in **Table IV**. The allometric coefficients for clearance (*a* and *b)* are generally consistent between these two methods. Compared to *NCA*, the mPBPK model fitting not only provides clearance values, but also provides a physiologically meaningful use of plasma volume and prediction of antibody distribution in two groups of lumped tissues (asbased on estimated σ_1 and σ_2). The σ_1 and σ_2 values shown in Figure 5 and listed in **Table III** demonstrate the differences in tissue distribution parameters among antibodies.

Based on the physiological and PK parameters estimated across animal species for erlizumab and canakinumab, simulations were conducted to predict the PK profiles in man (Figure 6). These case studies indicating how human profiles can be predicted by allometric scaling of preclinical data across species is provided as an example of utilizing the mAb mPBPK model to scale from preclinical animal experiments to man.

To further explore species differences in tissue distribution, the PK profiles were individually fitted for each species and the species-specific σ_1 and σ_2 values were estimated. Figures 7 and 8 summarize the predictions of *TER*, the equilibrium concentration ratios for tissues with tight endothelial junction (C_{tight}/C_{plasma}), and for tissues with leaky endothelium(C_{leaky}/C_{plasma}). Some antibodies exhibit similar extravasation rate (*TER*) and bio-distribution among species, such as trebananib and belimumab, while some show considerable species differences. Two-way ANOVA revealed that inter-species varability ($F = 1.58$, $p = 0.204$) for C_{tight}/C_{plasma} ratios is much smaller than inter-antibody variability ($F = 3.35$, $p = 0.004$), indicating higher predictabilities of bio-distribution into tight tissues are expected using species information than using antibody-averaged values. However, despite certain antibodies showing similar bio-distribution into tissues that have leaky endothelium (C_{leaky}/C_{plasma}), significant species differences of C_{leaky}/C_{plasma} ratios ($F = 1.39$, $p = 0.227$) were detected. Although monkey is normally thought to be the most suitable preclinical species, our analysis did not find greater similarity of monkey than other species for presumed bio-distribution.

DISCUSSION

Allometric scaling has been applied for large molecule drugs in some studies using *NCA* and compartmental model approaches. Mordenti (31) first applied allometric scaling for five therapeutic proteins showing that clearance could be well described using an allometric equation with the clearance exponent close to 0.75. Ling (32) found that simple allometric scaling using three species is useful for mAbs showing either linear kinetics over the tested dose range or receptor-mediated disposition only accounting for a small part of mAb disposition. Wang (4) confirmed that human *CL* can generally be predicted reasonably well with a fixed exponent of 0.8 in simple allometric scaling. Deng (1) demonstrated that using cynomolgus monkey PK data alone with a fixed scaling exponent of 0.85 could accurately predict mAb clearance in man. Our analysis indicated that the average scaling exponent for *CL* is around 0.90, but differs across antibodies.

The allometric exponent for *CL* varied with the modeling approach. This difference may be rooted theoretically. In an ideal situation with highly intensive sampling density, the minimal PBPK model-predicted *CL*, *NCA*-inferred *CL*, and compartmental model-predicted *CL* all should equal *Dose/AUC*. However, in practice, the physiological features of the minimal model such as initial dilution space (plasma volume) and tissue distribution mechanism (convection dominated), may make the model-predicted *AUC* slightly different than *NCA*-derived *AUC*, resulting a different estimation of *CL*. The *NCA* and compartment models both employ extrapolation for fitting of zero-time ($C_p(0)$) values, which may result in a biased *AUC*, particularly when initial sampling is scarce. The biased *AUC* may further give different predictions of clearance that would partly explain the different estimates of allometric exponents for *CL* (**Table IV**). The minimal PBPK model considers that antibodies poorly distribute into blood cells and assumes plasma volume as the initial dilution space. This assumption, also made in full PBPK models, adds greater certainty and stability in fittings of the initial PK decline phases.

One advantage of the mPBPK model is to provide physiologically relevant predictions of antibody distribution in two groups of lumped tissues. This was affirmed by comparisons with actual tissue concentrations from animal studies (15). The *NCA* or compartmental model approaches fit plasma profiles but reveal little about true tissue distribution for either small or large molecules.

In this model, only four parameters need to be estimated: vascular reflection coefficients σ_1 and σ_2, and the allometric slope (*a*) and exponent (*b*). For joint fittings, assuming all species share the same σ_1 and σ_2, we applied allometric scaling for 12 antibodies using the mPBPK modeling approach and obtained a mean *b* value of 0.91, with the range of 0.695 to 1.27. This differs from the mean value of 0.75 for small molecules and their wider distribution (0.3 to 1.2) (30). Using this mean exponent could be helpful for the prediction of clearance using the mAb mPBPK model when PK data from only one species are available.

The vascular reflection coefficients (σ_1 and σ_2) are specific distribution parameters for the mAb mPBPK model. They are not only associated with vascular permeability rates but also reflect the extent of distribution of mAb in tissues (16, 17). For joint fitting, the vascular reflection coefficients were assumed consistent across antibodies: σ_1 ranged 0.690 to 0.999 with an average of 0.908; σ_2 ranged 0.258 to 0.841 with an average of 0.579. Assuming the mean values simplifies this scaling approach leaving only clearance to be scaled across species. With this assumption, the model had a good performance for both joint fittings (Figure 3 and 4) and predictions from animals to man (Figure 6). In contrast, in our individual analysis, the vascular reflection coefficient σ_2 showed moderate inter-species variability (Figure 8).

The inconsistency between the joint and individual analysis may be related to computational issues. Firstly, joint fitting is more robust than fitting each species separately as more data produces greater certainty in the fitted parameters. Secondly, antibodies are known to have restricted tissue distribution and long blood persistence. These properties usually produce biexponential plasma profiles (Figures 3 and 4) with a short distribution phase (1-2 days) but a long terminal phase (often > 3 weeks). The overall *AUC* is primarily determined by the latter, while the initial phase is mainly associated with distribution properties. Thus, as long as plasma volume determines $C_p(0)$ and the clearance is well predicted, the model would reasonably characterize the overall profiles. Any bias in σ_1 and σ_2 values causes deviations in initial phase predictions. This is particularly true when there are limited early data. The insensitivity of the overall PK profiles for σ_1 and σ_2 may explain the discrepancy in our two stages of analysis. When assuming common σ_1 and σ_2 values across species in joint fittings, the PK profiles were reasonably captured by the mPBPK model. With the limited available data, this study showed that most antibodies could be handled with common σ_1 and σ_2 values. For greater clarity on antibody distribution, population-type data from many animals and more intensive early samplings are needed.

Multiple factors can influence mAb distribution and clearance including size, shape, charge, and hydrophobicity (33). An increase of net positive charge is associated with increased tissue retention and systemic clearance (34). A larger molecule generally exhibits less tissue penetration (35). These factors might account for different values of vascular reflection

coefficients among the mAbs. Data quality also reflects σ_1 and σ_2 as sparse data results in problems for their estimation. This model predicts antibody *ISF* concentrations based on analyzing plasma profiles only and direct measurements of *ISF* concentrations are needed for confirmation.

There are some limitations of this study due to the assumptions and data sources. Allometric scaling is based on the anatomical power relationship among species. However, species differences in the PK properties of mAbs could include FcRn-binding affinity, target density, as well as the local physiology of target-expressing tissues. Relevant data and evidence is lacking to address these potential limitations in the scaling of PK parameters. Besides insufficient data, factors that might also affect the allometric extrapolation include low numbers of animals and varying bio-analytical methods among different studies. Having specific lymph volumes and flows, ISF volumes, body weights, and other information for each species and study will also improve fittings and predictions.

In conclusion, this study integrated allometric scaling within a basic mPBPK model to successfully analyze the PK of 12 mAbs in several species. In joint analysis, with an assumption of conserved σ_1 and σ_2 across species, CL_p was scalable across species based on body weights. The biexponential plasma profiles were well predicted with this approach. Individual analysis for each species indicated possible inter-species variability of antibody distribution. Reasons for this discrepancy were assessed. This modeling approach, particularly with more extensive and specific data from animal studies, may be useful in species translation of PK and estimation of first-in human (FIH) doses.

Supplementary Material

Refer to Web version on PubMed Central for supplementary material.

ACKNOWLEDGMENTS

This research was supported by the National Institutes of Health Grant GM57980 and the UB Center for Protein Therapeutics.

Glossary

mPBPK	minimal physiologically based pharmacokinetic modeling
PBPK	physiologically based pharmacokinetic modeling
mAb	monoclonal antibody
PK	pharmacokinetic
FIH	first-in-human
BW	body weight
ISF	interstitial fluid
L	lymph flow
AIC	Akaike Information Criterion

SC	Schwarz Criterion
CV	Coefficient of variation
NCA	non-compartmental analysis
AUC	area under the plasma concentration-time curve

REFERENCES

1. Deng R, Iyer S, Theil FP, Mortensen DL, Fielder PJ, Prabhu S. Projecting human pharmacokinetics of therapeutic antibodies from nonclinical data: What have we learned? MAbs. 2011; 3(1):61–66. [PubMed: 20962582]
2. Wang W, Wang EQ, Balthasar JP. Monoclonal antibody pharmacokinetics and pharmacodynamics. Clinical Pharmacology and Therapeutics. 2008; 84(5):548–558. [PubMed: 18784655]
3. Mordenti J. Man versus beast: pharmacokinetic scaling in mammals. Journal of Pharmaceutical Sciences. 1986; 75(11):1028–1040. [PubMed: 3820096]
4. Wang W, Prueksaritanont T. Prediction of human clearance of therapeutic proteins: simple allometric scaling method revisited. Biopharmaceutics & Drug Disposition. 2010; 31(4):253–263. [PubMed: 20437464]
5. Ritschel WA, Vachharajani NN, Johnson RD, Hussain AS. The allometric approach for interspecies scaling of pharmacokinetic parameters. Comparative Biochemistry and Physiology C, Comparative Pharmacology and Toxicology. 1992; 103(2):249–253.
6. Duconge J, Fernandez-Sanchez E, Alvarez D. Interspecies scaling of the monoclonal anti-EGF receptor ior EGF/r3 antibody disposition using allometric paradigm: is it really suitable? Biopharmaceutics & Drug Disposition. 2004; 25(4):177–186. [PubMed: 15108220]
7. Boxenbaum H, Fertig JB. Scaling of antipyrine intrinsic clearance of unbound drug in 15 mammalian species. European Journal of Drug Metabolism and Pharmacokinetics. 1984; 9(2):177–183. [PubMed: 6745307]
8. Mahmood I, Balian JD. Interspecies scaling: predicting clearance of drugs in humans. Three different approaches. Xenobiotica; the fate of foreign compounds in biological systems. 1996; 26(9):887–895.
9. Lave T, Coassolo P, Reigner B. Prediction of hepatic metabolic clearance based on interspecies allometric scaling techniques and in vitro-in vivo correlations. Clinical Pharmacokinetics. 1999; 36(3):211–231. [PubMed: 10223169]
10. Bischoff KB, Dedrick RL, Zaharko DS. Preliminary model for methotrexate pharmacokinetics. Journal of Pharmaceutical Sciences. 1970; 59(2):149–154. [PubMed: 5411336]
11. Baxter LT, Zhu H, Mackensen DG, Jain RK. Physiologically based pharmacokinetic model for specific and nonspecific monoclonal antibodies and fragments in normal tissues and human tumor xenografts in nude mice. Cancer Research. 1994; 54(6):1517–1528. [PubMed: 8137258]
12. Baxter LT, Zhu H, Mackensen DG, Butler WF, Jain RK. Biodistribution of monoclonal antibodies: scale-up from mouse to human using a physiologically based pharmacokinetic model. Cancer Research. 1995; 55(20):4611–4622. [PubMed: 7553638]
13. Davda JP, Jain M, Batra SK, Gwilt PR, Robinson DH. A physiologically based pharmacokinetic (PBPK) model to characterize and predict the disposition of monoclonal antibody CC49 and its single chain Fv constructs. International Immunopharmacology. 2008; 8(3):401–413. [PubMed: 18279794]
14. Mann S, Droz PO, Vahter M. A physiologically based pharmacokinetic model for arsenic exposure. II. Validation and application in humans. Toxicology and Applied Pharmacology. 1996; 140(2):471–486. [PubMed: 8887465]
15. Cao Y, Balthasar JP, Jusko WJ. Second-generation minimal physiologically-based pharmacokinetic model for monoclonal antibodies. Journal of Pharmacokinetics and Pharmacodynamics. 2013; 40(5):597–607. [PubMed: 23996115]

16. Cao Y, Jusko WJ. Survey of monoclonal antibody disposition in man utilizing a minimal physiologically-based pharmacokinetic model. Journal of Pharmacokinetics and Pharmacodynamics. 2014; 41(6):571–580. [PubMed: 25146360]
17. Cao Y, Jusko WJ. Incorporating target-mediated drug disposition in a minimal physiologically-based pharmacokinetic model for monoclonal antibodies. Journal of Pharmacokinetics and Pharmacodynamics. 2014; 41(4):375–387. [PubMed: 25077917]
18. Pang KS, Rowland M. Hepatic clearance of drugs. I. Theoretical considerations of a “well-stirred” model and a “parallel tube” model. Influence of hepatic blood flow, plasma and blood cell binding, and the hepatocellular enzymatic activity on hepatic drug clearance. Journal of Pharmacokinetics and Biopharmaceutics. 1977; 5(6):625–653. [PubMed: 599411]
19. Shah DK, Betts AM. Towards a platform PBPK model to characterize the plasma and tissue disposition of monoclonal antibodies in preclinical species and human. Journal of Pharmacokinetics and Pharmacodynamics. 2012; 39(1):67–86. [PubMed: 22143261]
20. Rossing N. Intra- and extravascular distribution of albumin and immunoglobulin in man. Lymphology. 1978; 11(4):138–142. [PubMed: 739785]
21. Boxenbaum H. Interspecies pharmacokinetic scaling and the evolutionary-comparative paradigm. Drug Metabolism Reviews. 1984; 15(5-6):1071–1121. [PubMed: 6396053]
22. Porter CJ, Edwards GA, Charman SA. Lymphatic transport of proteins after s.c. injection: implications of animal model selection. Advanced Drug Delivery Reviews. 2001; 50(1-2):157–171. [PubMed: 11489338]
23. Lindena J, Kupper W, Trautschold I. Catalytic enzyme activity concentration in thoracic duct, liver, and intestinal lymph of the dog, the rabbit, the rat and the mouse. Approach to a quantitative diagnostic enzymology, II. Communication. *J Clin Chem Clin Biochem*.. 1986; 24(1):19–33. [PubMed: 3701268]
24. Davies B, Morris T. Physiological parameters in laboratory animals and humans. Pharmaceutical Research. 1993; 10(7):1093–1095. [PubMed: 8378254]
25. Rodionov, N. Graph digitizer version 1.9.2000. 2000. http://www.geocities.com/graphdigitizer
26. D’Argenio, DZ.; Schumitzky, A. ADAPT V user’s guide: pharmacokinetic/pharmacodynamic systerm analysis software, Biomedical Simulations Resorce. Los Angeles, CA: 2009.
27. Vugmeyster Y, Szklut P, Tchistiakova L, Abraham W, Kasaian M, Xu X. Preclinical pharmacokinetics, interspecies scaling, and tissue distribution of humanized monoclonal anti-IL-13 antibodies with different IL-13 neutralization mechanisms. International Immunopharmacology. 2008; 8(3):477–483. [PubMed: 18279802]
28. Lin YS, Nguyen C, Mendoza JL, Escandon E, Fei D, Meng YG, Modi NB. Preclinical pharmacokinetics, interspecies scaling, and tissue distribution of a humanized monoclonal antibody against vascular endothelial growth factor. The Journal of Pharmacology and Experimental Therapeutics. 1999; 288(1):371–378. [PubMed: 9862791]
29. Garg A, Balthasar JP. Physiologically-based pharmacokinetic (PBPK) model to predict IgG tissue kinetics in wild-type and FcRn-knockout mice. Journal of Pharmacokinetics and Pharmacodynamics. 2007; 34(5):687–709. [PubMed: 17636457]
30. Tang H, Mayersohn M. A novel model for prediction of human drug clearance by allometric scaling. Drug Metabolism and Disposition. 2005; 33(9):1297–1303. [PubMed: 15958605]
31. Mordenti J, Chen SA, Moore JA, Ferraiolo BL, Green JD. Interspecies scaling of clearance and volume of distribution data for five therapeutic proteins. Pharmaceutical Research. 1991; 8(11): 1351–1359. [PubMed: 1798669]
32. Ling J, Zhou H, Jiao Q, Davis HM. Interspecies scaling of therapeutic monoclonal antibodies: initial look. Journal of Clinical Pharmacology. 2009; 49(12):1382–1402. [PubMed: 19837907]
33. Bumbaca D, Boswell CA, Fielder PJ, Khawli LA. Physiochemical and biochemical factors influencing the pharmacokinetics of antibody therapeutics. The AAPS Journal. 2012; 14(3):554–558. [PubMed: 22610647]
34. Boswell CA, Tesar DB, Mukhyala K, Theil FP, Fielder PJ, Khawli LA. Effects of charge on antibody tissue distribution and pharmacokinetics. Bioconjugate Chemistry. 2010; 21(12):2153–2163. [PubMed: 21053952]

35. Schmidt MM, Wittrup KD. A modeling analysis of the effects of molecular size and binding affinity on tumor targeting. Molecular Cancer Therapeutics. 2009; 8(10):2861–2871. [PubMed: 19825804]

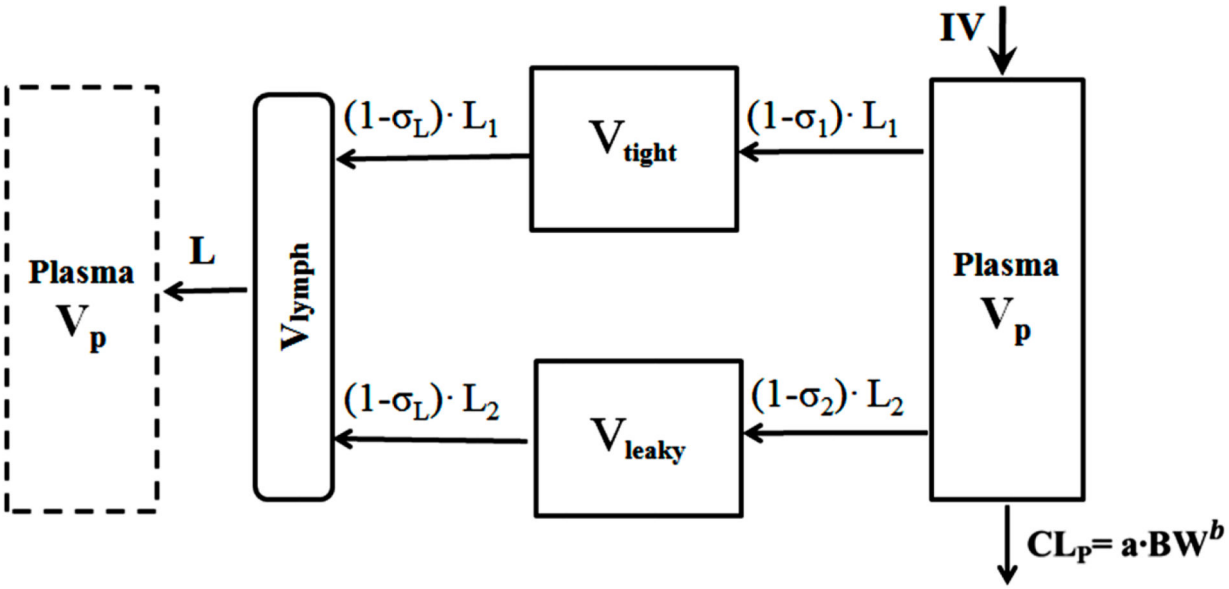

Figure 1.

The mAb minimal PBPK model with allometric scaling of systemic clearance (CL_p). Symbols and physiological restrictions are defined with Eq (1-4). The left box represents the venous plasma as in full PBPK models, but is not applied in the present model.

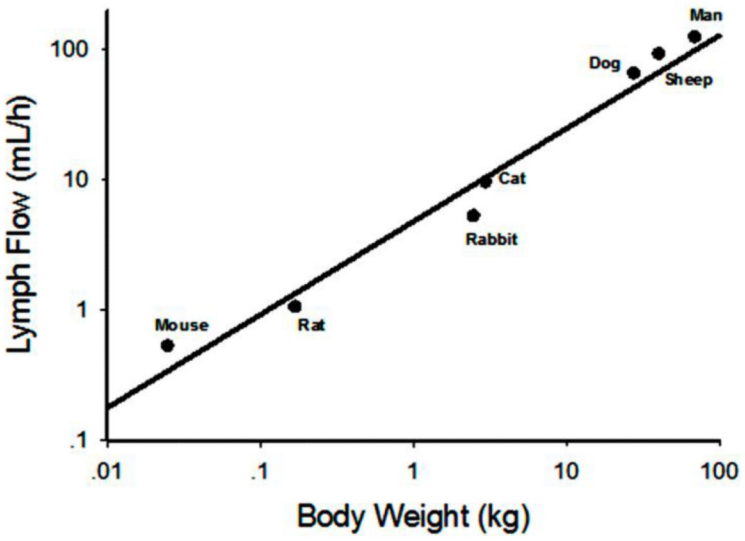

Figure 2.

Allometric relationship between total lymph flow and species body weights. Mouse, rat, rabbit, cat, dog, and man data were extracted from Lindena *et al* (23). Sheep data were obtained from Porter *et al* (22). The regression line is $Lymph\ Flow = 4.92 \cdot BW^{0.730}$

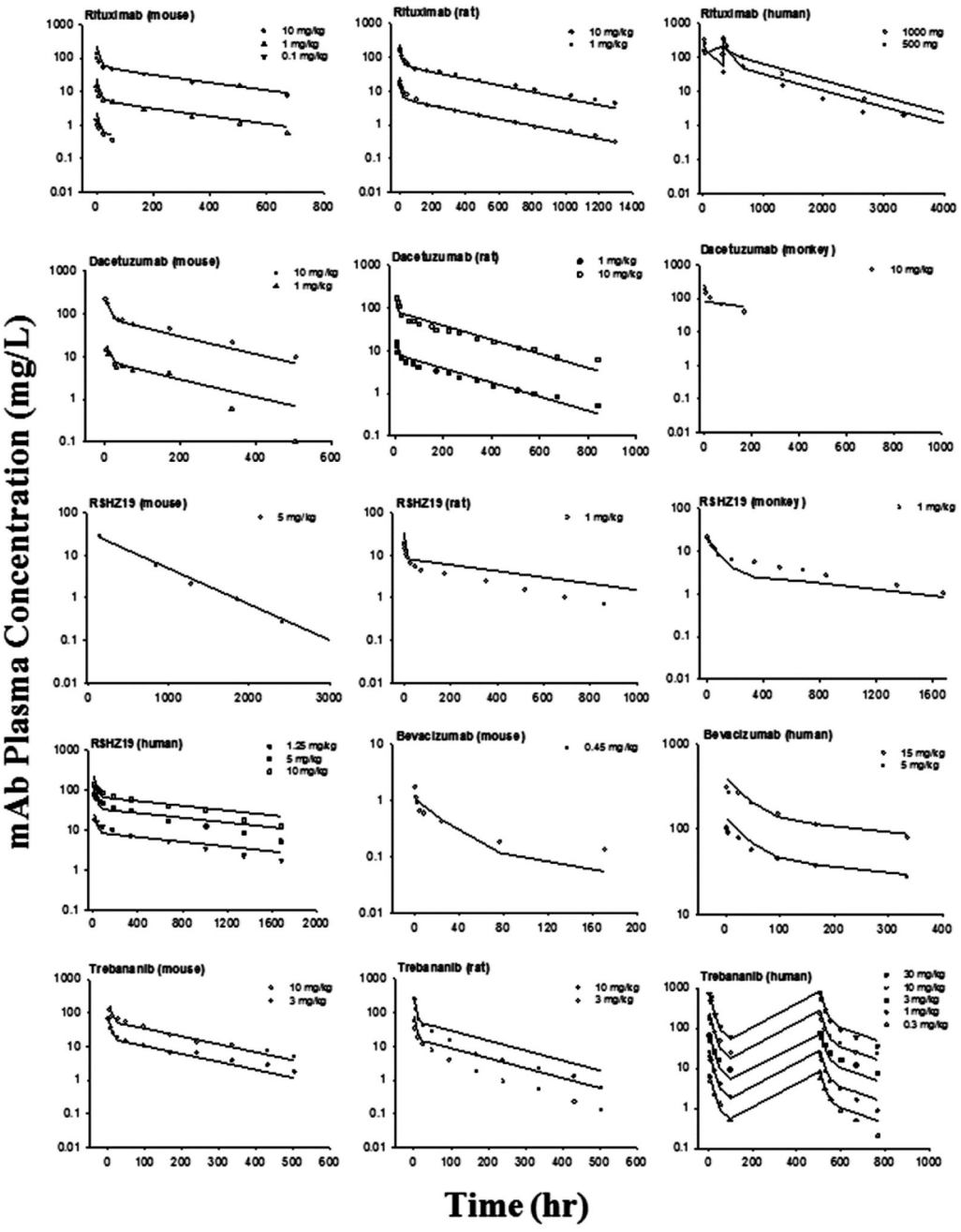

Figure 3.

Pharmacokinetic profiles of 5 mAbs across species. Symbols are observations and curves are model fittings.

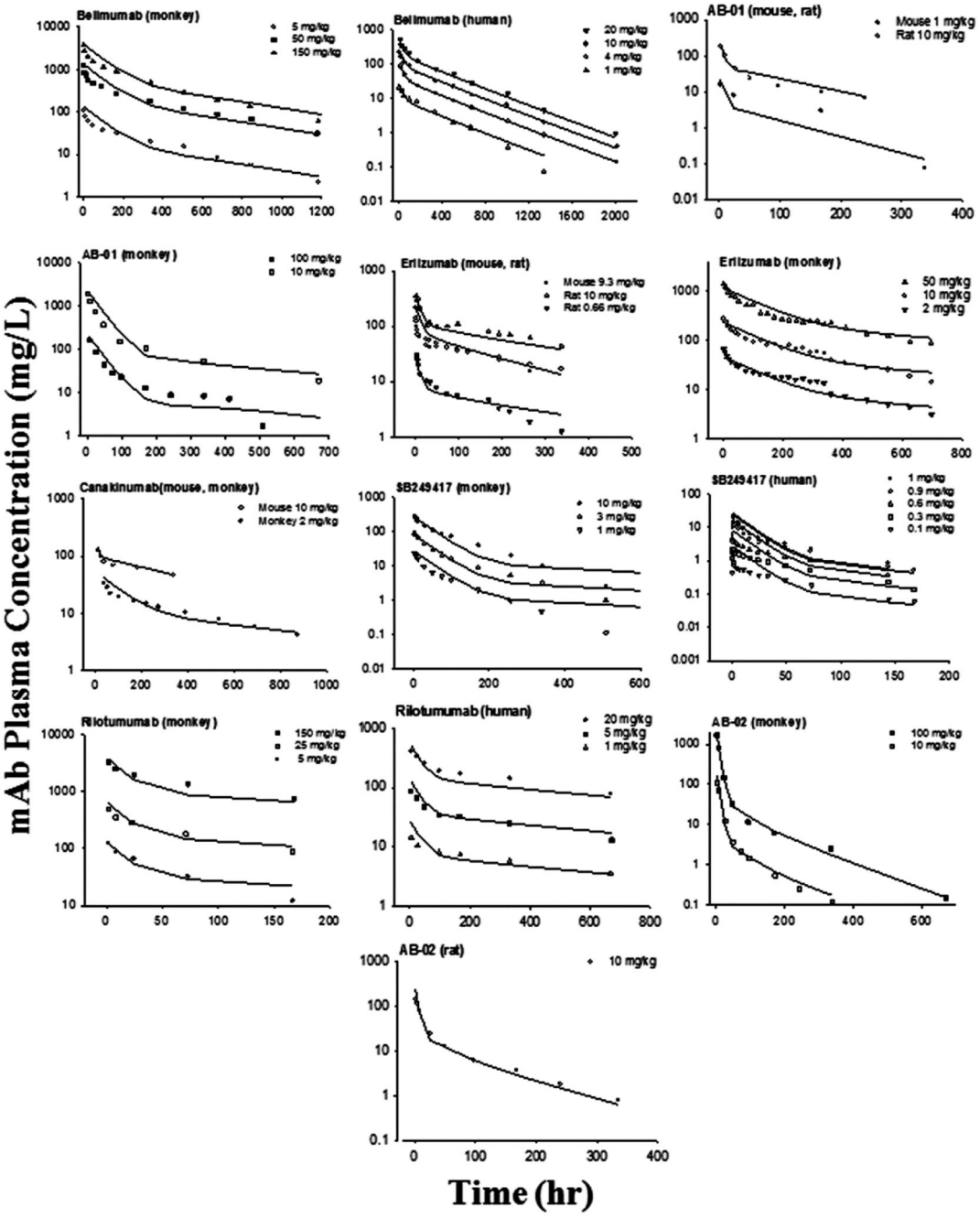

Figure 4.

Pharmacokinetic profiles of 7 mAbs across species. Symbols are observations and curves are model fittings.

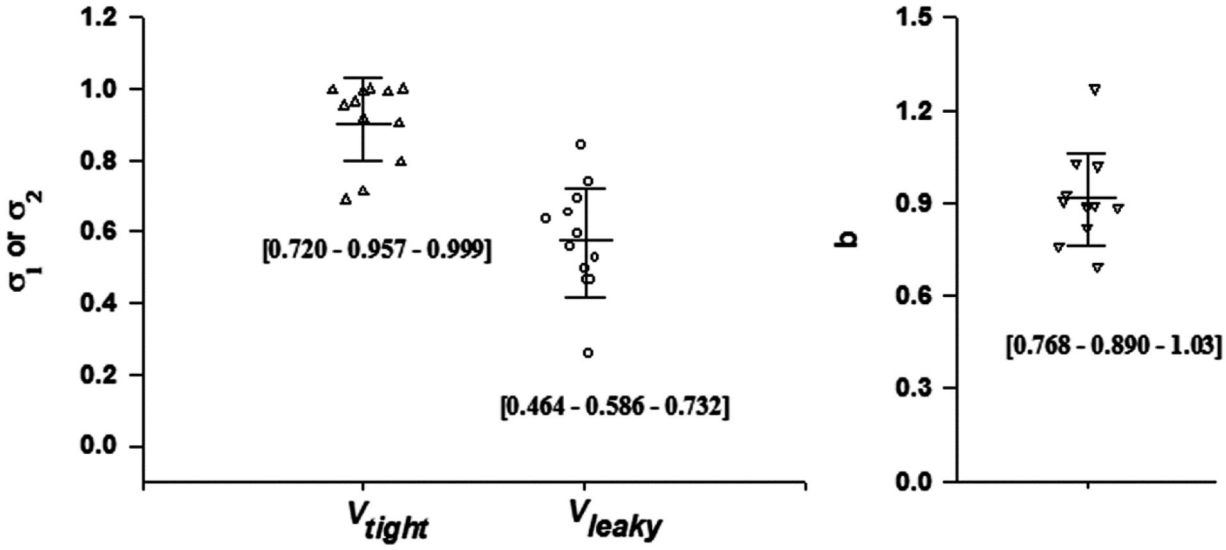

Figure 5.

The estimated parameters of 12 mAbs using the mAb minimal PBPK model with allometric scaling of CL_p providing reflection coefficients (σ_1 and σ_2) for two groups of tissues (V_{tight} and V_{leaky}) and allometric exponents (b). Bars represent mean and standard deviation. Numbers in brackets are [10% - 50% - 90%] percentiles.

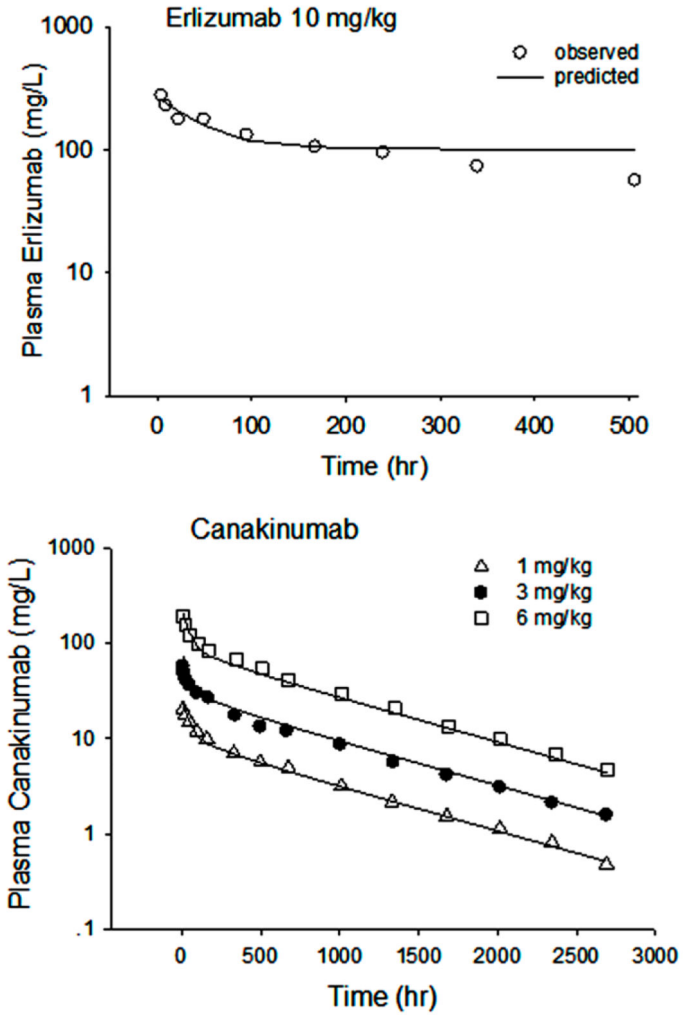

Figure 6.

Predictions of human PK profiles of erlizumab and canakinumab from animal data, where erlizumab used mouse, rat and monkey data and canakinumab used mouse and monkey data. Symbols are observations and curves are model simulations.

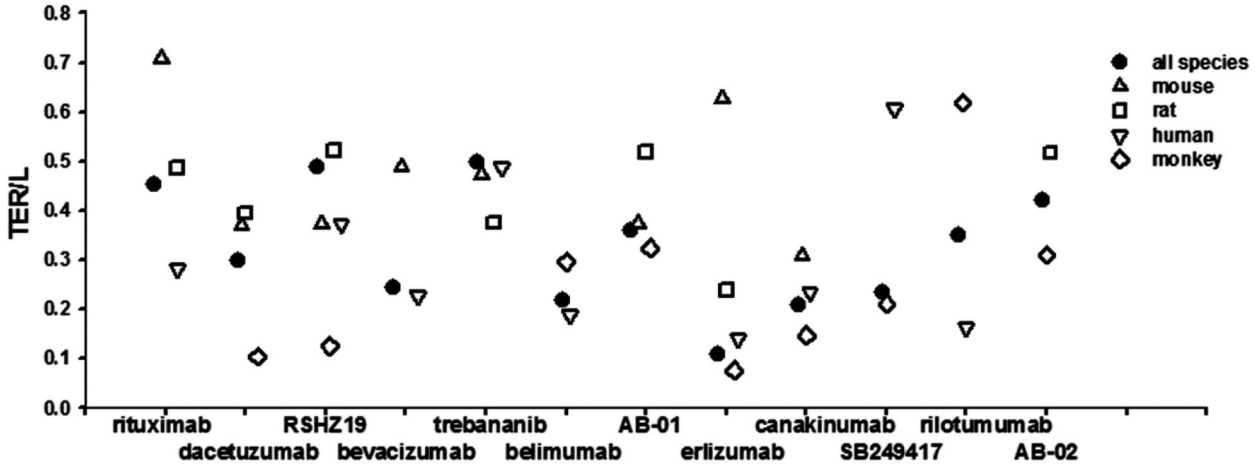

Figure 7.

Transcapillary extravascular rate/lymph flow (*TER/L*) for each antibody obtained by joint fitting all species and individual fitting each species. Two-way ANOVA revealed a significant effect of species on *TER/L* ($F = 3.36$, $p = 0.022$), but no significant effect of antibody on *TER/L* ($F = 1.42$, $p = 0.216$).

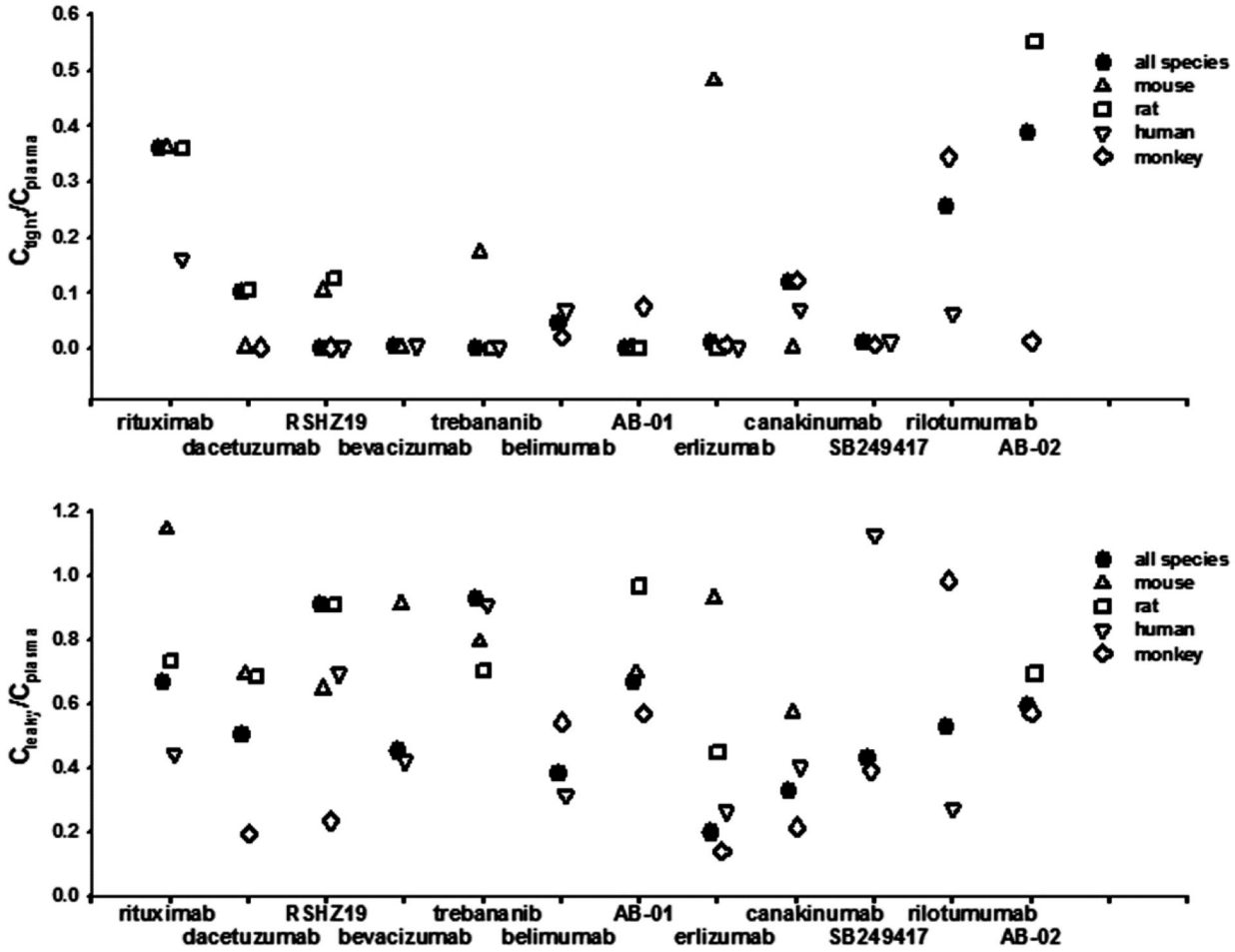

Figure 8.

C_{tight}/C_{plasma} and C_{leaky}/C_{plasma} ratios at equilibrium for each antibody obtained by joint and individual fitting each species. Two-way ANOVA revealed a significant effect of the antibody on C_{tight}/C_{plasma} ($F = 3.35$, $p = 0.004$), but no significant effect of the species on C_{tight}/C_{plasma} ($F = 1.58$, $p = 0.204$). For C_{leaky}/C_{plasma} at equilibrium, no significant effect of antibody on the C_{leaky}/C_{plasma} ($F = 1.39$, $p = 0.227$) but a significant effect of species on C_{leaky}/C_{plasma} ($F = 3.03$, $p = 0.0331$).

Table I

Physiological parameters used for scaling of lymph flow and PK properties of 12 mAbs across species.

	Man	Sheep	Dog	Monkey	Cat	Rabbit	Rat	Mouse
Body weight, kg	70	40.8	28	3.5	3.0	2.5	0.3	0.020
Thoracic duct [a], ml/h/kg	1.38	1.82	1.88	NA	2.56	1.68	4.10	4.80
Lymph flow, ml/h/kg	1.73	2.27	2.35	3.51	3.20	2.10	5.13	6.00
ISF, L	15.6	NA	NA	0.735	NA	NA	0.0699	0.00435
Lymph volume (V_{lymph}), L	5.2	NA	NA	0.314	NA	NA	0.0162	0.0016
Plasma (V_p), L	2.6	NA	NA	0.157	NA	NA	0.0081	0.00085

NA: not applicable

[a] Thoracic duct data for mouse, rat, rabbit, cat, dog, and man were extracted from Lindena et al (23). Thoracic duct data for Sheep were obtained from Porter et al (22).

Table II

The 12 mAbs analyzed using the mPBPK model with allometric scaling

Compound (Ref[b])	Source	Binding target	Species
Rituximab (S1,S2)	chimeric IgG_1	CD20	mouse, rat, human
Dacetuzumab (S3)	humanized IgG_1	CD40	mouse, rat, monkey
RSHZ19 (S4-6)	humanized IgG_1	RSV	mouse, rat, monkey, human
Bevacizumab (S7,S8)	humanized IgG_1	VEGF	mouse, human
Trebananib (S9,S10)	peptibody	ANG-1/ ANG-2	mouse, rat, human
Belimumab (S11,S12)	human IgG_1	BAFF, BL_yS	monkey, human
AB-01(S13,S14)	human	IL-13	mouse, rat, monkey
Erlizumab(S15,S16)	humanized IgG_1	VEGF	mouse, rat, monkey, human
Canakinumab(S17)	humanized IgG_1	IL-1β	mouse, monkey, human
SB249417(S18,S19)	humanized IgG_1	IX/IX_a	monkey, human
Rilotumumab(S20,S21)	human IgG_2	HGF	monkey, human
AB-02 (S14,S22)	humanized IgG_1	IL-13	monkey, rat

[b] References provided in supplementary materials

Table III

Estimated pharmacokinetic parameters (*CV*%) for 12 mAbs

Compound	Reflection Coefficients		Allometric Factors	
	σ_1	σ_2	a (10^{-4} L/h)	b
Rituximab	0.712 (12.0)	0.467 (8.58)	3.02 (5.15)	0.888 (1.40)
Dacetuzumab	0.917 (18.0)	0.596 (30.2)	2.81 (31.8)	0.820 (24.3)
RSHZ19	0.952 (16.2)	0.497 (21.4)	1.85 (12.5)	0.906 (5.10)
Bevacizumab	0.995 (0.199)	0.637 (21.3)	4.07 (38.0)	0.762 (11.4)
Trebananib	0.999 (<0.01)	0.258 (11.1)	8.90 (1.68)	1.02 (0.536)
Belimumab	0.963 (4.66)	0.694 (3.84)	2.32 (12.8)	1.03 (4.63)
AB-01	0.999 (<0.01)	0.464 (43.6)	8.08 (32.7)	0.893 (13.7)
Erlizumab	0.990 (9.05)	0.841 (12.1)	2.61 (3.18)	0.844 (1.56)
Canakinumab	0.903 (9.08)	0.737 (10.2)	1.69 (5.70)	0.885 (2.39)
SB249417	0.990 (<0.01)	0.654 (8.04)	4.86 (10.3)	1.27(2.56)
Rilotumumab	0.796 (<0.01)	0.577(<0.01)	4.71 (<0.01)	0.695 (<0.01)
AB-02	0.690 (43.7)	0.526 (41.1)	23.4 (8.32)	0.929 (6.76)

Table IV

Comparisons of *CL* between non-compartmental analysis and mPBPK model fitting

	Non-compartmental analysis						mPBPK		Comparison
Compound	**Mouse**	**Rat**	**Monkey**	**Human**	**Equation**	**Prediction CL_{human}**	**Equation**	**Prediction CL_{human}**	***Ratio of Prediction human CL***
	CL(×10^{-4} L/h/kg)				**(×10^{-4} L/h)**	**(×10^{-4} L/h/kg)**	**(×10^{-4} L/h)**	**(×10^{-4} L/h/kg)**	**$CL_{NCA\ human}$/ $CL_{mPBPK\ human}$**
Dacetuzumab	4.58-7.05	4.61-4.58	5.17	NA	$CL=4.87\times BW^{0.975}$	4.38	$CL=2.81\times BW^{0.820}$	1.31	3.34
Rituximab	5.16-18.2	3.17-3.43	NA	44.8-49.2	$CL=11.5\times BW^{1.24}$	31.8	$CL=3.02\times BW^{0.888}$	1.87	17.0
RSHZ19	2.49	3.96	1.43	1.19-1.35	$CL=2.06\times BW^{0.886}$	1.26	$CL=1.64\times BW^{0.867}$	0.92	1.36
Bevacizumab	72.2	NA	NA	1.40-1.80	$CL=11.5\times BW^{0.532}$	1.57	$CL=4.07\times BW^{0.762}$	1.48	1.06
Trebananib	7.04-7.63	17.4-20	NA	1.16-12.1	$CL=5.72\times BW^{0.783}$	2.28	$CL=8.90\times BW^{1.02}$	9.68	0.24
Belimumab	NA	NA	2.48-2.77	2.44-2.72	$CL=2.58\times BW^{1.00}$	2.58	$CL=2.32\times BW^{1.03}$	2.63	0.99
AB-01	7.65	17.3	9.51-11.3	NA	$CL=11.1\times BW^{1.02}$	12.1	$CL=8.08\times BW^{0.893}$	5.13	2.35
Erlizumab	6.39	2.39-3.52	2.32-2.48	1.17	$CL=2.64\times BW^{0.821}$	1.23	$CL=2.61\times BW^{0.844}$	1.35	0.91
Canakinumab	2.04	NA	1.56	1.01	$CL=1.54\times BW^{0.918}$	1.09	$CL=1.69\times BW^{0.885}$	1.03	1.05
SB249417	NA	NA	4.72-7.83	21.4-27.2	$CL=3.22\times BW^{1.46}$	22.7	$CL=4.86\times BW^{1.27}$	15.3	1.48
Rilotumumab	NA	NA	4.26-6.56	1.23-1.94	$CL=9.48\times BW^{0.563}$	1.48	$CL=4.71\times BW^{0.695}$	1.29	1.14
AB-02	NA	28.1	44.1-51.0	NA	$CL=37.7\times BW^{1.18}$	80.9	$CL=23.4\times BW^{0.929}$	17.3	4.67

NA: not applicable